International Journal of Emerging Technology and Advanced Engineering
Website: www.ijetae.com (E-ISSN 2250-2459, Scopus Indexed, ISO 9001:2008 Certified Journal, Volume 12, Issue 06, June 2022)
Manuscript Received: 18 April 2022, Received in Revised form: 22 May 2022, Accepted: 29 May 2022 DOI: 10.46338/ijetae0622_18

Third-Order Robust Fuzzy Sliding Mode Tracking Control of a Double-Acting Electrohydraulic Actuator

Muhammad Fadli Ghani[1], Rozaimi Ghazali[2], Hazriq Izzuan Jaafar[3], Chong Chee Soon[4], Yahaya Md. Sam[5], Zulfatman Has[6]

[1]Malaysian Institute of Marine Engineering Technology (MIMET), Universiti Kuala Lumpur, 32200, Lumut, Perak, Malaysia
[2,3,4]Centre for Robotics and Industrial Automation, Faculty of Electrical Engineering, Universiti Teknikal Malaysia Melaka, Hang Tuah Jaya, 76100, Durian Tunggal, Melaka, Malaysia
[5]Department of Control and Mechatronics Engineering, School of Electrical Engineering, Universiti Teknologi Malaysia, 81310 Skudai, Johor, Malaysia
[6]Electrical Engineering Department, University of Muhammadiyah Malang, 65144 Malang, Indonesia

***Abstract*— In the industrial sector, an electrohydraulic actuator (EHA) system is a common technology. This system is often used in applications that demand high force, such as the steel, automotive, and aerospace industries. Furthermore, since most mechanical actuators' performance changes with time, it is considerably more difficult to assure its robustness over time. Therefore, this paper proposed a robust fuzzy sliding mode proportional derivative (FSMCPD) controller. The sliding mode controller (SMC) is accomplished by utilizing the exponential law and the Lyapunov theorem to ensure closed loop stability. By replacing the fuzzy logic control (FLC) function over the signum function, the chattering in the SMC controller has been considerably reduced. By using the sum of absolute errors as the objective function, particle swarm optimization (PSO) was used to optimize the controller parameter gain. The experiment results for trajectory tracking and the robustness test were compared with the sliding mode proportional derivative (SMCPD) controller to demonstrate the performance of the FSMCPD controller. According to the findings of the thorough study, the FSMCPD controller outperforms the SMCPD controller in terms of mean square error (MSE) and robustness index (RI).**

***Keywords*—tracking control, electrohydraulic actuator (EHA), robust control design, fuzzy sliding mode proportional derivative (FSMCPD), particle swarm optimization (PSO).**

I. INTRODUCTION

Because of their compact size in proportion to their power, strong force producing capabilities, and rapid response times, electrohydraulic actuator (EHA) systems are particularly practical and reliable.

These features make them attractive in construction equipment, sometimes called mobile hydraulic machines, where they are often used [1]–[6]. While the EHA system is known to be a nonlinear system with substantial uncertainties due to the servo valve's high-frequency behavior and external disturbances, it is also known to be a nonlinear system with considerable uncertainties. Furthermore, the presence of uncertainties, nonlinearities, and disturbances in the EHA system usually results in tracking errors and phase lag during the trajectory tracking process, increasing the difficulty of controller design [3], [7]–[14]. These problems make researchers think about how to improve the EHA's performance.

In this work, two types of controllers are principally addressed: a sliding mode proportional derivative (SMCPD) controller and a fuzzy sliding mode proportional derivative (FSMCPD) controller. Because the SMC is only limited by practical restrictions on the amplitude of the control signals it produces, it can theoretically cope with a broad range of uncertainties as well as limited external disturbances. SMC.

The purpose of this research is to present the implementation of FSMCPD controller on a third-order model of a double-acting EHA system. The SMC control has been improved with the addition of a PD sliding surface to increase the performance of the EHA system's trajectory tracking. The Lyapunov criteria are used to demonstrate the stability of the proposed control strategy. Experimenting and comparing the performance of the proposed control methodology to SMCPD controller has shown the utility of the proposed control methodology. The following is a breakdown of the contributions made by the paper:

International Journal of Emerging Technology and Advanced Engineering
Website: www.ijetae.com (E-ISSN 2250-2459, Scopus Indexed, ISO 9001:2008 Certified Journal, Volume 12, Issue 06, June 2022)

a) The FSMCPD controller is presented and successfully demonstrated for effective robust control on a third order model of a double-acting EHA system for trajectory tracking under the influence of supply pressure Consequently, conventional SMCs are typically constructed with a discontinuous switching function. The inaccuracy of the switching operation will result in unpleasant chattering [49]–[57]. During the reaching phase, a fuzzy logic control function is utilized to replace the discontinuous signum function used in conventional variations.

b) Chattering was significantly reduced when the suggested controller's optimized settings were adjusted. This was accomplished by employing the PSO technique to acquire the optimized parameters.

Furthermore, this paper is structured as follows: Section II discusses the current literature. Section III presents the dynamical model of a double-acting EHA system and optimization. Section IV explains how the suggested sliding mode control was developed. Section V presents the experiment findings for the performance of a double-acting electrohydraulic actuator system. Section VI focuses on the performance and potential expansion of the planned control.

II. Literature Review

Numerous solutions have been suggested to solve the current challenges, with a focus on the establishment of robust control systems to overcome uncertainties, system parameter variation, and disturbances. To cope with the EHA system's complexity and challenges, an intelligent and effective control method will be required. Different types of control approaches have been discovered in the literature during the last decades, in the application of the challenges in the tracking control of EHA systems. A growing number of works on EHA system control have been proposed, ranging from linear control and nonlinear control to intelligent control strategies like generalized predictive control (GPC) [15]–[17], model reference adaptive control (MRAC) [18]–[20], sliding mode control (SMC) [21]–[26], self-tuning fuzzy proportional-integral-derivative (PID) [27]–[30], and neural network (NN) [31]–[36]. The SMC control approach has been shown to have high potential and is frequently used in the EHA system.

The SMC, a nonlinear control approach based on variable order models, has been effectively used to the regulation of nonlinear and uncertain systems.

It was widely utilized and extremely successful in the control of nonlinear complex systems. A variety of technical applications, including active suspension systems [37]–[41], pneumatic systems [42]–[47], and active magnetic bearing systems [48], have benefited from the SMC's capabilities.

III. Modelling And Optimization

A. System Identification

The system identification, which entails modeling the system using sets of input and output data, either with or without previous knowledge of the system's operation. In current work, the model structure estimation is constructed using a mathematical derivation based on the EHA system shown in Fig. 1 and by neglecting non-linearity parameters such as internal or external leakage and valve dynamics [58], the symbols for which are displayed in Table I.

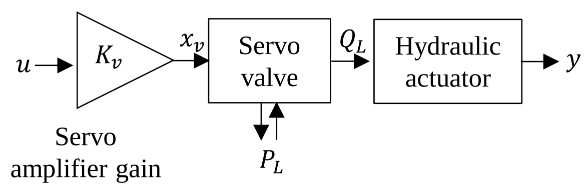

Fig. 1 The EHA system for model structure estimation.

TABLE I
Representation of the Symbols

Symbol	Representation
u	Input signal
x_v	Spool valve position
K_v	Servo valve gain
Q_L	Total oil flow
K_q	Flow-gain coefficient
P_L	Load pressure
K_c	Flow-pressure coefficient
β_e	Effective bulk modulus
V_t	Total oil volume
C_{tp}	Total leakage coefficient
A_p	Surface area of the piston
y	Piston position
F_a	Actuator force
M_t	Total mass

International Journal of Emerging Technology and Advanced Engineering
Website: www.ijetae.com (E-ISSN 2250-2459, Scopus Indexed, ISO 9001:2008 Certified Journal, Volume 12, Issue 06, June 2022)

Eq. (1) defines the association between the input signal, the servo valve gain, and the spool valve position, and Eq. (2) describes the relationship between the overall oil flows dynamics of the EHA system derived from a Taylor series linearization. Furthermore, Eq. (3) indicates the load pressure deviations over time.

$$x_v = K_v u \tag{1}$$

$$Q_L = K_q x_v - K_c P_L \tag{2}$$

$$\dot{P}_L = \frac{4\beta_e}{V_t}(Q_L - C_{tp}P_L - A_p\dot{y}) \tag{3}$$

As a result, the force produced by the actuator from a total mass coupled to the piston's end is characterized as

$$F_a = A_p P_L = M_t \ddot{y} \tag{4}$$

Substituting Eqs. (2) and (3) into the derivative of Eq. (4) produces

$$M_t\dddot{y} + M_t\ddot{y}\frac{4\beta_e}{V_t}(K_c + C_{tp}) + {A_p}^2\frac{4\beta_e}{V_t}\dot{y} = A_p\frac{4\beta_e}{V_t}K_q K_v u \tag{5}$$

Let $b_1 = A_p \frac{4\beta_e}{M_t V_t} K_q K_v$, $b_2 = \frac{4\beta_e}{V_t}(K_c + C_{tp})$ and $b_3 = {A_p}^2 \frac{4\beta_e}{M_t V_t}$ the Eqn. (5) becomes,

$$\dddot{y} = u a_1 - a_2\ddot{y} - a_3\dot{y} \tag{6}$$

Taking a Laplace transform on Eq. (6) becomes

$$\frac{Y(s)}{U(s)} = \frac{b_1}{s(s^2 + b_2 s + b_3)} \tag{7}$$

In this work, the dynamical model of the double-acting EHA system with $8{\times}10^3$ kPa supply pressure is developed. The time domain input-output data collected by the experimental hardware and software arrangement presented in Fig. 2 is utilized to determine the continuous transfer function.

The arrangement has a computer unit installed with MATLAB and SIMULINK software; a data acquisition system (DAQ) system with power supply unit, and a hydraulic plant consist of hydraulic power pack, a proportional valve (Bosch Rexroth 4WREE 6 E08-2X/G24K31/A1V), and a hydraulic actuator (Bosch Rexroth – 200 mm single-rod double acting cylinder) attached with wire displacement sensor. Furthermore, the MATLAB/System identification toolbox is utilized to get a transfer function parameter based on Eq. (7) that matches the detailed model by examining the collection of input and output data.

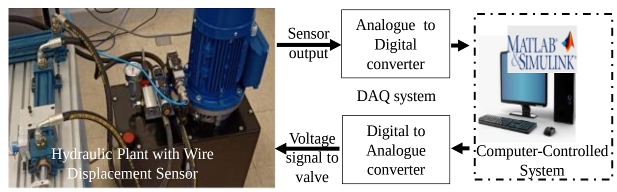

Figure 2. Experimental hardware and software arrangement for system identification.

B. Particle Swarm Optimization

The PSO can be employed to obtain finest values of the design gain parameters and its algorithm was designed by mimicking the swarm social behaviour of bird flocking and fish schooling. A swarm of individuals called particle move through a high-dimensional search space among the entire population towards the global optimal (minimum or maximum) solution with a specific position and velocity. Each particle in the swarm offers a great solution and adheres to a simple principle by replicating its own previous success [52], [59].

Furthermore, the personal best position in a neighbourhood influences the position of particle and the optimal solution among the personal best positions is known as the global best position. Essentially, the PSO algorithm's implementation may be described as shown in Fig. 3. In the current work, the particle population size, maximum iteration, and cognitive and social coefficients are all set to 20, 50, 2, and 2, respectively.

International Journal of Emerging Technology and Advanced Engineering
Website: www.ijetae.com (E-ISSN 2250-2459, Scopus Indexed, ISO 9001:2008 Certified Journal, Volume 12, Issue 06, June 2022)

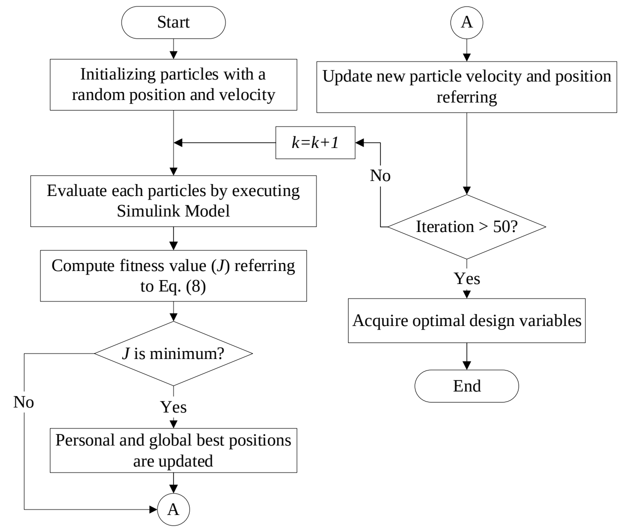

Figure 3. Common process of the PSO algorithm.

$$J = \sum |e(t)| \tag{8}$$

IV. Controllers Design

This section describes the design of the SMCPD and FSMCPD controllers. The SMC is a model-based control system in which the output of the controller is built differently for each system under the controller's control. According to the Lyapunov stability theory, the design technique guarantees that the system will persist stable under any conditions [10], [28], [60]–[65].

A. SMCPD Controllers

In this section the fundamental design of the SMCPD controller is presented. The signal of error, *e* is specified as

$$e = r - y \tag{9}$$

where *r* is the signal of desired trajectory. Then, the 3rd differentiation of Eq. (9) turns out to be

$$\dddot{e} = \dddot{r} - \dddot{y} \tag{10}$$

In this work, the proportional and derivative sliding surface, s for third order EHA system is considered as

$$s = \left(k_p + k_d \frac{d}{dt}\right)^{n-1} e \tag{11}$$

where n is the order of EHA system, Eq. (11) becomes

$$s = k_p^2 e + 2k_P k_d \dot{e} + k_d^2 \ddot{e} \tag{12}$$

Then, the differentiation of Eq. (12) becomes

$$\dot{s} = k_p^2 \dot{e} + 2k_P k_d \ddot{e} + k_d^2 \dddot{e} \tag{13}$$

Combining Eq. (10), Eq. (13) becomes

$$\dot{s} = k_p^2 \dot{e} + 2k_P k_d \ddot{e} + k_d^2(\dddot{r} - \dddot{y}) \tag{14}$$

With the use of a reaching law, the system output is compelled to follow the surface under consideration. In order to guarantee the stability of the closed loop system, the reaching law must be developed in such a manner that it meets certain criteria. The exponential law [66], as shown in Eq. (15), is used in the proposed investigation.

$$\dot{s} = -\epsilon sgn(s) - ks;\ \epsilon > 0, k > 0 \tag{15}$$

where ε and k are constants. Then, solving for Eq. (6), (14) and (15), the control signal of SMCPD is denoted as

$$u_{SMCPD} = \frac{k_p^2}{a_1 k_d^2}\dot{e} + \frac{2k_p}{a_1 k_d}\ddot{e} + \frac{1}{a_1}(\dddot{r} + a_2\ddot{y} + a_3\dot{y}) + \frac{1}{a_1 k_d^2}(\epsilon sgn(s) + ks) \tag{16}$$

B. FSMCPD Controller

In this section the vital design of the FSMCPD controller is presented. When the SMC controller is functioned, it causes a fast oscillation phenomenon known as "chattering" at the controller output due to a discontinuity in the signum function that arises during control action. In order to overcome this difficulty, the fuzzy logic control (FLC) denotes as $fuzz(s)$ is employed in the present work instead of the signum function.

$$\begin{aligned} fuzz(s) > 0;\quad & s > 0 \\ fuzz(s) = 0;\quad & s = 0 \\ fuzz(s) < 0;\quad & s < 0 \end{aligned} \tag{17}$$

$$\dot{s} = -\epsilon fuzz(s) - ks;\ \epsilon > 0, k > 0$$

A single-input and single-output FLC has been utilized where the sliding surface is used as input. Three triangular input membership functions (MFs) were used, as shown in Fig. 4, which denoted as Negative Input (NI), Zero Input (ZI), and Positive Input (PI).

International Journal of Emerging Technology and Advanced Engineering
Website: www.ijetae.com (E-ISSN 2250-2459, Scopus Indexed, ISO 9001:2008 Certified Journal, Volume 12, Issue 06, June 2022)

Meanwhile, three output MFs which denoted as Negative Output (NO), Zero Output (ZO), and Positive Output (PO) were used, as shown in Fig. 5. Table II presents the utilized rule base which has been considered from Eq. (17). Mamdani type min-max inference and the center of gravity defuzzification method have been used in the present work.

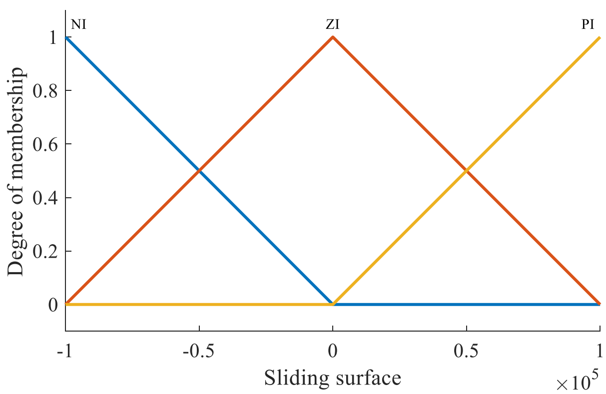

Figure 4. Input membership functions of FLC.

The resulting control action of input output profile is shown in Fig. 6 which implies the rule base design. Then, solving for Eqs. (6), (14) and (17), the control signal of FSMCPD is denoted as

$$u_{FSMCPD} = \frac{k_p^2}{a_1 k_d^2}\dot{e} + \frac{2k_p}{a_1 k_d}\ddot{e} + \frac{1}{a_1}(\dddot{r} + a_2\ddot{y} + a_3\dot{y}) + \frac{1}{a_1 k_d^2}(\epsilon fuzz(s) + ks) \quad (18)$$

TABLE II
INPUT-OUTPUT RULE BASE FOR FLC

Input	NI	ZI	PI
Output	NO	ZO	PO

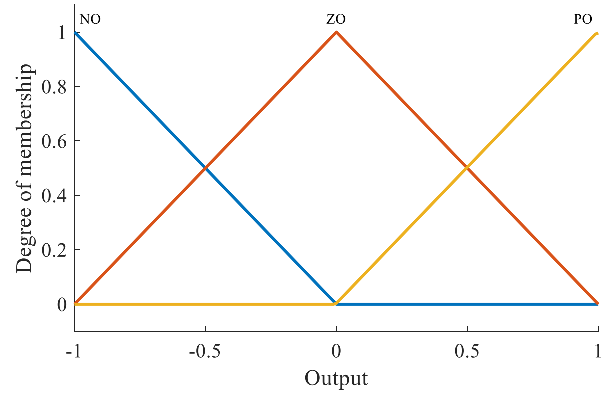

Figure 5. Output membership functions of FLC.

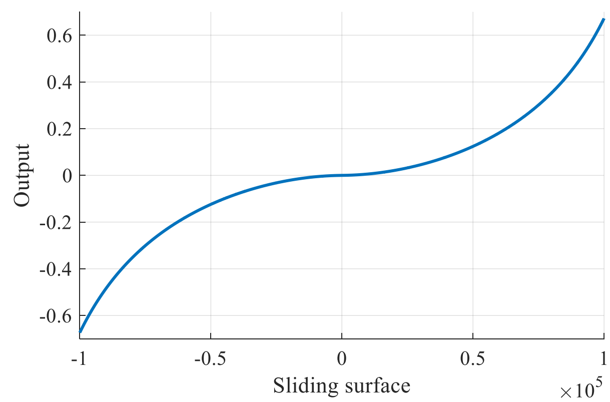

Figure 6. Input-output surface plot of FLC.

C. Stability Analysis using Lyapunov Criteria: SMCPD

The crucial aim of SMC controller design is to ensure that the feedback control system is always stable in its overall operation. It is predicted by the Lyapunov stability theorem that when the condition $s\dot{s} < 0$ is satisfied, the whole system will be stable and will approach the sliding surface. In this present work, the Lyapunov function is denoted as

$$V = \frac{1}{2}s^2 \quad (19)$$

$$\dot{V} = s\dot{s} \quad (20)$$

Substituting Eq. (15) into Eq. (20) becomes

$$\dot{V} = -s(\epsilon sgn(s) + ks);\ \varepsilon > 0, k > 0 \qquad (21)$$

When $s > 0$ and $sgn(s) > 0$, Eq. (21) becomes

$$\dot{V} = -s(\epsilon sgn(s) + ks) < 0 \qquad (22)$$

When $s < 0$ and $sgn(s) < 0$, Eq. (21) becomes

$$\dot{V} = -s(\epsilon sgn(s) + ks) < 0 \qquad (23)$$

As revealed by Eq. (22), $\dot{V} < 0$, which states that the design controller for the exponential reaching rule will be stable for s > 0. Furthermore, Eq. (23) showed that $\dot{V} < 0$, which affirms that the design controller for the exponential reaching rule will be stable for s < 0. Based on Eq. (22) and (23), the Lyapunov stability theory is being used to guide the design of SMCPD controller for third-order double-acting EHA systems, and the system output will be bound when the input is bounded.

D. Stability Analysis using Lyapunov Criteria: FSMCPD

Substituting Eq. (17) into Eq. (20) becomes,

$$\dot{V} = -s(\epsilon fuzz(s) + ks);\ \varepsilon > 0, k > 0 \qquad (24)$$

When $s > 0$ and $fuzz(s) > 0$, Eq. (21) becomes,

$$\dot{V} = -s(\epsilon fuzz(s) + ks) < 0 \qquad (25)$$

When $s < 0$ and $fuzz(s) < 0$, Eq. (21) becomes,

$$\dot{V} = -s(\epsilon fuzz(s) + ks) < 0 \qquad (26)$$

As revealed by Eq. (25), $\dot{V} < 0$, which states that the design controller for the exponential reaching rule will be stable for s > 0. Furthermore, Eq. (26) showed that $\dot{V} < 0$, which asserts that the design controller for the exponential reaching rule will be stable for s < 0. Based on Eq. (25) and (26), the Lyapunov stability theory is being used to guide the design of SMCPD controller for third-order double-acting EHA systems, and the system output will be bound when the input is bounded.

E. Performance Evaluation Criteria

i. *Mean Square Error (MSE)*: MSE disqualifies large-valued errors over small-valued errors, which reflect overshoot and aggressive control. In the current work, the magnitude of chattering phenomenon is reflected relatively proportional to the MSE magnitude.

$$MSE = \frac{1}{n}\sum_{t=0}^{T}\left(e(t)\right)^2 \qquad (27)$$

ii. *Robustness Index (RI)*: The robustness test is practiced assessing the robustness of the established controller. Commonly, robustness test for the EHA system is conducted by reducing or increasing the supply pressure to characterize the parameter variations. The examinations under variations of the operating conditions and robustness study of the employed controllers are vital in control performance evaluation. Accordingly, an applied approach to measure the robustness of the controllers is by determining the MSE for the nominal operating condition (NOM) and under the changed of plant parameters (VAR). In the current work, the robustness and adaptive tests are conducted at 8×10^3 kPa as nominal supply pressure with three variations of supply pressure: 6×10^3 kPa as variation 1 (VAR1), 4×10^3 kPa as variation 2 (VAR2), and 2×10^3 kPa as variation 3 (VAR3). The numerical measure which known as the *RI* for a reference trajectory, under a particular plant condition, and over a tracking process of period is given as

$$RI = \frac{|MSE(NOM) - MSE(VAR)|}{MSE(NOM)} \qquad (28)$$

V. Experiment Results And Discussion

The assessment of tracking control performance for the SMCPD and FSMCPD controllers are conducted using MATLAB/Simulink (R2021b) with 1 ms of sampling time and optimized parameters using PSO is shown in this section. In addition, the chaotic signal is used to generate the required trajectory. The chaotic trajectory tracking consists of sinusoidal and point-to-point trajectories which is composed together.

IJETAE
EXPLORING RESEARCH AND INNOVATIONS

International Journal of Emerging Technology and Advanced Engineering

Website: www.ijetae.com (E-ISSN 2250-2459, Scopus Indexed, ISO 9001:2008 Certified Journal, Volume 12, Issue 06, June 2022)

In the experimental study, chaotic trajectory tracking performance of the SMCPD and FSMCPD controllers are assessed which have the fast and slow velocity to accomplish high tracking performance for alteration set points of trajectory throughout the actuator stroke. The values of b_1, b_2, and b_3 are 144400, 3.723, and 7855, respectively, which are developed by the system identification procedure. Furthermore, the values of k_p, k_d, ϵ, and k are 259.2978, 1, 3.0788, and 10.9706, respectively, which are developed by the PSO process. A systematic investigation was carried out, and the results are shown in Table III, where the mean square error (*MSE*) and robustness index (*RI*) values are calculated. Meanwhile, in Figs. 7–12, a trajectory tracking task, the related controller output, and error curves are shown, confirming the dominance of the FSMCPD controller over the SMCPD in terms of performance and accuracy.

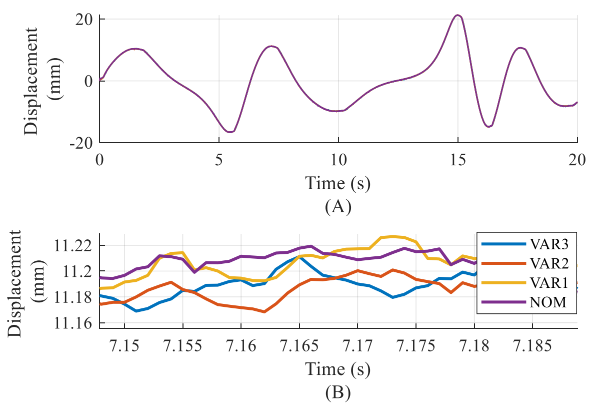

Figure 7. Output performance of SMCPD; (A) Origin and (B) zoom.

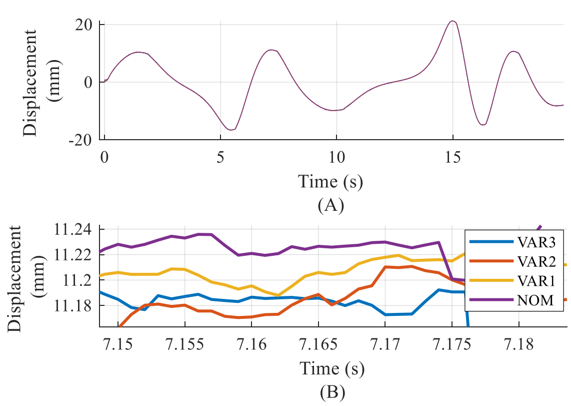

Figure 8. Output performance of FSMCPD; (A) Origin and (B) zoom.

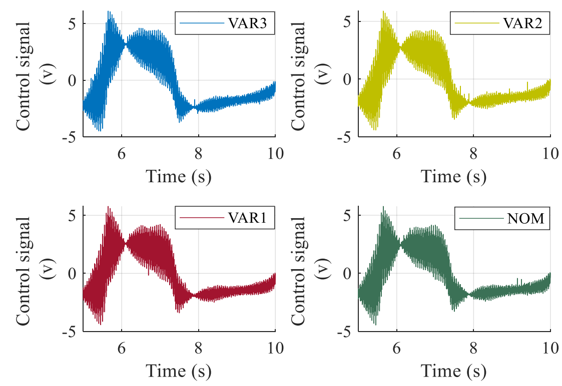

Figure 9. Control signal of SMCPD.

The FSMC delivers more appropriate and improved performance in trajectory tracking control based on MSE analyses, controller efforts, and tracking performance clarifications. In Fig. 13, the sliding surface shows that the system has arrived the sliding phase and will stay there until it reaches the stability point, at which point the error and derivative of error approach zero even in the variation of supply pressure.

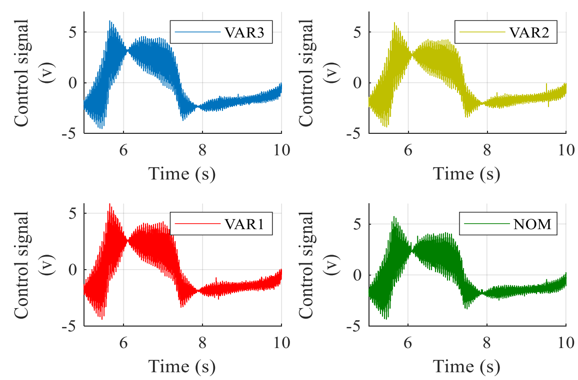

Figure 10. Control signal of FSMCPD.

International Journal of Emerging Technology and Advanced Engineering
Website: www.ijetae.com (E-ISSN 2250-2459, Scopus Indexed, ISO 9001:2008 Certified Journal, Volume 12, Issue 06, June 2022)

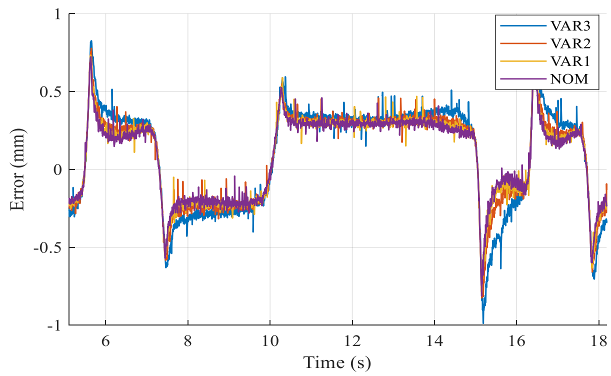

Figure 11. Error signal of SMCPD.

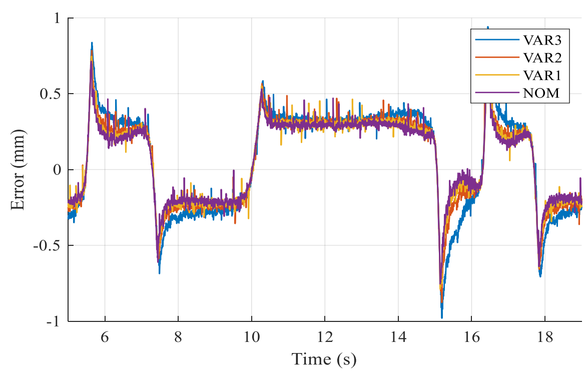

Figure 12. Error signal of FSMCPD.

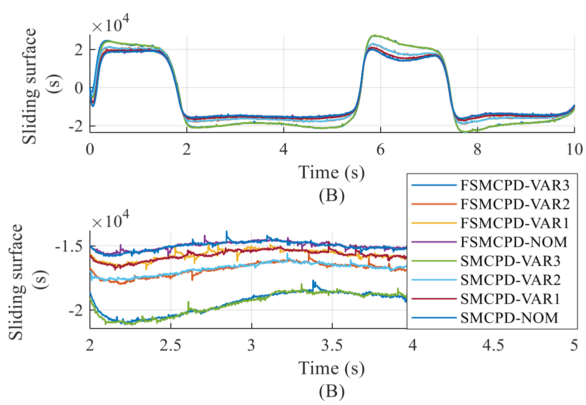

Figure 13. Sliding surface signals; (A) Origin and (B) zoom.

TABLE III
MSE AND RI FOR CHAOTIC TRAJECTORY

CONTROLLER	*MSE* (×10^{-2})				*RI* (×10^{-2})		
	NOM	VAR 1	VAR 2	VAR 3	VAR 1	VAR 2	VAR 3
SMCPD	6.86	7.45	8.48	11.43	8.60	23.62	66.62
FSMCPD	6.85	7.43	8.46	11.36	8.47	23.50	65.84

VI. CONCLUSION

It is shown in this paper that nonlinear double-acting electrohydraulic actuator (EHA) systems can be controlled using sliding mode proportional derivative (SMCPD) controller, as well as fuzzy sliding mode proportional derivative (FSMCPD) controller. The performance of controllers is evaluated in the context of trajectory tracking tasks and robustness tests, respectively. Chattering is a key problem that must be handled in a traditional sliding mode controller (SMC). This issue is solved by substituting the signum function with a Fuzzy Logic Control (FLC) function. The SMC controllers are built with exponential law which ensuring that the entire system is stable based on Lyapunov's law. The sum of square errors was used to calculate the overall performance index. PSO oversees tuning the gains of the controllers. The experimented results obtained indicate that the FSMCPD controller outperforms the SMCPD controller in all the performance characteristics tested throughout the controller assessment process. It is necessary to test the performance of various SMC versions, such as fractional order sliding mode proportional derivative and fractional order fuzzy sliding mode proportional derivative controllers, which may be explored further based on in this work.

Acknowledgement

The support of Universiti Teknikal Malaysia Melaka (UTeM), Universiti Kuala Lumpur (UniKL) and Ministry of Education (MOE) are greatly acknowledged. The research was funded by Fundamental Research Grant Scheme (FRGS) Grant No. FRGS/1/2021/FKE/F00468.

REFERENCES

[1] Niu, Z., Liu, Y., Wang, L., Yang, S., & Li, X. 2016. Portable electro-hydraulic actuator technology based on spherical micro pump. 2016 IEEE International Conference on Aircraft Utility Systems (AUS), 114–118.

International Journal of Emerging Technology and Advanced Engineering
Website: www.ijetae.com (E-ISSN 2250-2459, Scopus Indexed, ISO 9001:2008 Certified Journal, Volume 12, Issue 06, June 2022)

[2] Lee, D., Song, B., Park, S. Y., & Baek, Y. S. (2019). Development and Control of an Electro-Hydraulic Actuator System for an Exoskeleton Robot. Applied Sciences, 9(20), 4295.

[3] Jovanovic, V., Djuric, A., Karanovic, V., & Stevanov, B. (2016, March). Applications of electro-hydraulics actuators. In SoutheastCon 2016 (pp. 1-5). IEEE.

[4] Tamburrano, P., Plummer, A. R., Distaso, E., & Amirante, R. (2019). A Review of Direct Drive Proportional Electrohydraulic Spool Valves: Industrial State-of-the-Art and Research Advancements. Journal of Dynamic Systems, Measurement, and Control, 141(2).

[5] Yang, M., Wang, C., Qi, Z., Wang, X., Yu, H., Zhong, Y., Zhang, H., Xi, R., & Sun, Z. (2018). Design and Model Analysis of a Robotic Joint with Circular Electro-hydraulic Actuator. 2018 3rd International Conference on Advanced Robotics and Mechatronics (ICARM), 520–525.

[6] Jiang, J., Wang, Y., Cao, H., Zhu, J., & Zhang, X. (2020). A novel pump-valve coordinated controlled hydraulic system for the lower extremity exoskeleton. Transactions of the Institute of Measurement and Control, 42(15), 2872–2884.

[7] Tomov, P., & Yanulov, D. (2020). Modelling and Examining the Dynamic Characteristics of an Electro-Hydraulic Unit for Discrete Control Based on Direct Acting High-Speed Servo Valve. 2020 21st International Symposium on Electrical Apparatus & Technologies (SIELA), 1–4.

[8] Kim, J.-H., & Hong, Y.-S. (2020). Improvement of Backdrivability of a Force-Controlled EHA by Introducing Bypass Flow Control. International Journal of Precision Engineering and Manufacturing, 21(5), 819–830.

[9] Huang, J., An, H., Lang, L., Wei, Q., & Ma, H. (2020). A Data-Driven Multi-Scale Online Joint Estimation of States and Parameters for Electro-Hydraulic Actuator in Legged Robot. IEEE Access, 8(2), 36885–36902.

[10] Yang, M., Ma, K., Shi, Y., & Wang, X. (2019). Modeling and Position Tracking Control of a Novel Circular Hydraulic Actuator With Uncertain Parameters. IEEE Access, 7, 181022–181031.

[11] Ding, R., Zhang, J., Xu, B., & Cheng, M. (2018). Programmable hydraulic control technique in construction machinery: Status, challenges and countermeasures. Automation in Construction, 95, 172–192.

[12] Mahato, A. C., & Ghoshal, S. K. (2021). Energy-saving strategies on power hydraulic system: An overview. Proceedings of the Institution of Mechanical Engineers, Part I: Journal of Systems and Control Engineering, 235(2), 147–169.

[13] Yoo, S., Lee, W., & Chung, W. K. (2019). Impedance Control of Hydraulic Actuation Systems With Inherent Backdrivability. IEEE/ASME Transactions on Mechatronics, 24(5), 1921–1930.

[14] Yang, G., & Yao, J. (2020). Nonlinear adaptive output feedback robust control of hydraulic actuators with largely unknown modeling uncertainties. Applied Mathematical Modelling, 79, 824–842.

[15] Wong Liang, X., Mohd Faudzi, A. 'Athif, & Ismail, Z. H. (2019). System Identification and Model Predictive Control using CVXGEN for Electro-Hydraulic Actuator. International Journal of Integrated Engineering, 11(4), 166–174.

[16] Emhemed, A. A., Mamat, R. B., Johary, M. R., & Osman, K. (2016). Modified Predictive Control for a Class of Electro-Hydraulic Actuator. International Journal of Electrical and Computer Engineering (IJECE), 6(2), 630–638.

[17] Edge, K. A. (1997). The control of fluid power systems-responding to the challenges. Proceedings of the Institution of Mechanical Engineers, Part I: Journal of Systems and Control Engineering, 211(2), 91–110.

[18] Kireçci, A., Topalbekiroglu, M., & Eker, I. (2003). Experimental evaluation of a model reference adaptive control for a hydraulic robot: a case study. Robotica, 21, 71–78.

[19] Yifei Zhao, & Zongxia Jiao. (2016). Fractional model reference adaptive control for electro-hydraulic servo system. 2016 IEEE Chinese Guidance, Navigation and Control Conference (CGNCC), 2048–2052.

[20] Alqadasi, M. M. A., Othman, S. M., Rahmat, M. F., & Abdullah, F. (2019). Optimization of PID for industrial electro-hydraulic actuator using PSOGSA. TELKOMNIKA (Telecommunication Computing Electronics and Control), 17(5), 2625.

[21] Utkin, V., & Lee, H. (2006). Chattering Problem in Sliding Mode Control Systems. In IFAC Proceedings Volumes (Vol. 39, Issue 5).

[22] Chen, Z., Yuan, X., Yuan, Y., Lei, X., & Zhang, B. (2019). Parameter estimation of fuzzy sliding mode controller for hydraulic turbine regulating system based on HICA algorithm. Renewable Energy, 133, 551–565.

[23] Yang, M., Zhang, Q., Lu, X., Xi, R., & Wang, X. (2019). Adaptive Sliding Mode Control of a Nonlinear Electro-hydraulic Servo System for Position Tracking. Mechanics, 25(4), 283–290.

[24] Nemati, H., Bandala, M., Albrecht, O. L. R., & Taylor, C. J. (2020). Reduced Chatter Sliding Mode Control for Hydraulic Manipulators based on Continuous-Time State Dependent Parameter Models. 2020 Australian and New Zealand Control Conference (ANZCC), November, 125–130.

[25] Ianagui, A. S. S., & Tannuri, E. A. (2018). High Order Sliding Mode Control and Observation for DP Systems. IFAC-PapersOnLine, 51(29), 110–115.

[26] Tony Thomas, A., Parameshwaran, R., Sathiyavathi, S., & Vimala Starbino, A. (2019). Improved Position Tracking Performance of Electrohydraulic Actuator Using PID and Sliding Mode Controller. IETE Journal of Research, 0(0), 1–13.

[27] Wang, H., Wang, X., Huang, J., Wang, J., & Quan, L. (2018). A Novel Control Strategy for Pilot Controlled Proportional Flow Valve with Internal Displacement-Flow Feedback. Journal of Dynamic Systems, Measurement, and Control, 140(11), 1–9.

[28] Li, X., Zhu, Z.-C., Rui, G.-C., Cheng, D., Shen, G., & Tang, Y. (2018). Force Loading Tracking Control of an Electro-Hydraulic Actuator Based on a Nonlinear Adaptive Fuzzy Backstepping Control Scheme. Symmetry, 10(5), 155.

[29] Kumar, J., Kumar, V., & Rana, K. (2018). Design of robust fractional order fuzzy sliding mode PID controller for two link robotic manipulator system. Journal of Intelligent & Fuzzy Systems, 35(5), 5301–5315.

[30] Han, C., Choi, S. B., & Han, Y. M. (2018). A piezoelectric actuator-based direct-drive valve for fast motion control at high operating temperatures. Applied Sciences (Switzerland), 8(10).

[31] Jelali, M., & Andreas, K. (2002). Hydraulic servo-systems: modelling, identification and control. Springer Science & Business Media.

[32] Cisneros, N., Rojas, A. J., & Ramirez, H. (2020). Port-Hamiltonian Modeling and Control of a Micro-Channel Experimental Plant. IEEE Access, 8, 176935–176946.

[33] Yang, X., Zheng, X., & Chen, Y. (2018a). Position Tracking Control Law for an Electro-Hydraulic Servo System Based on Backstepping and Extended Differentiator. IEEE/ASME Transactions on Mechatronics, 23(1), 132–140.

[34] Zong-Yi, X., Qiang, G., Li-Min, J., & Ying-Ying, W. (2008). Modelling and identification of electrohydraulic system and its application. IFAC Proceedings Volumes, 41(2), 6446-6451.

[35] Guo, Q., & Chen, Z. (2021). Neural adaptive control of single-rod electrohydraulic system with lumped uncertainty. Mechanical Systems and Signal Processing, 146, 106869.

[36] Yang, X., Zheng, X., & Chen, Y. (2018b). Position Tracking Control Law for an Electro-Hydraulic Servo System Based on Backstepping and Extended Differentiator. IEEE/ASME Transactions on Mechatronics, 23(1), 132–140.

[37] Du, M., Zhao, D., Ni, T., Ma, L., & Du, S. (2020). Output Feedback Control for Active Suspension Electro-hydraulic Actuator Systems with a Novel Sampled-data Nonlinear Extended State Observer. IEEE Access, 8, 1–1.

[38] Kou, F., Wang, Z., Du, J., Li, D., & Fan, E. (2017). Study on force tracking control of electro-hydraulic active suspension. 2017 IEEE 3rd Information Technology and Mechatronics Engineering Conference (ITOEC), 6(1), 1078–1082.

[39] Sam, Y. M., Osman, J. H. S., & Ghani, M. R. a. (2004). A class of proportional-integral sliding mode control with application to active suspension system. Systems and Control Letters, 51, 217–223.

[40] Wang, D., Zhao, D., Gong, M., & Yang, B. (2018). Research on Robust Model Predictive Control for Electro-Hydraulic Servo Active Suspension Systems. IEEE Access, 6, 3231–3240.

[41] Nemeth, B., Fenyes, D., Gaspar, P., & Bokor, J. (2017). Control design of an electro-hydraulic actuator for variable-geometry suspension systems. 2017 25th Mediterranean Conference on Control and Automation (MED), 180–185.

[42] Pan, Q., Zeng, Y., Li, Y., Jiang, X., & Huang, M. (2021). Experimental investigation of friction behaviors for double-acting hydraulic actuators with different reciprocating seals. Tribology International, 153(June 2020), 106506.

[43] Hyon, S.-H., Taniai, Y., Hiranuma, K., Yasunaga, K., & Mizui, H. (2019). Overpressure Compensation for Hydraulic Hybrid Servo Booster Applied to Hydraulic Manipulator. IEEE Robotics and Automation Letters, 4(2), 942–949.

[44] Ligang, H., YaoXing, S., Zongxia, J., Shuai, W., & Xiaobin, L. (2018, June). Simulation study of EHA with four-quadrant energy regulation based on hydraulic damping valve scheme. In CSAA/IET International Conference on Aircraft Utility Systems (AUS 2018) (pp. 1-8). IET.

[45] Banerjee, P., & Pandey, K. (2016). Implementation of Failure Modes and Effect Analysis on the electro-hydraulic servo valve for steam turbine. 2016 IEEE 1st International Conference on Power Electronics, Intelligent Control and Energy Systems (ICPEICES), 1–3.

[46] Yan, X., & Chen, B. (2021). Analysis of a novel energy-efficient system with 3-D vertical structure for hydraulic press. Energy, 218, 119518.

[47] Zhang, Q., Kong, X., Yu, B., Ba, K., Jin, Z., & Kang, Y. (2020). Review and Development Trend of Digital Hydraulic Technology. Applied Sciences, 10(2), 579.

[48] Salleh, S., Rahmat, M. F., Othman, S. M., & Danapalasingam, K. A. (2015). Review on modeling and controller design of hydraulic actuator systems. International Journal on Smart Sensing and Intelligent Systems, 8(1), 338–367.

[49] GGhani, M. F., Ghazali, R., Jaafar, H. I., Soon, C. C., Shern, C. M., & Has, Z. (2021, August). The Effects of Mass Variation on Closed-loop EHA System under High Leakage Flow Condition. In 2021 11th IEEE International Conference on Control System, Computing and Engineering (ICCSCE) (pp. 206-209). IEEE.

[50] Soon, C. C., Ghazali, R., Ghani, M. F., Shern, C. M., Sam, Y. M., & Has, Z. (2020). Tracking Analysis for an Optimized Robust Controller in Hydraulic System. ARPN Journal of Engineering and Applied Sciences, 15(23), 2800–2805.

[51] Shern, C. M., Ghazali, R., Horng, C. S., Soon, C. C., Ghani, M. F., Sam, Y. M., & Has, Z. (2021). The Effects of Weightage Values with Two Objective Functions in iPSO for Electro-Hydraulic Actuator System. Journal of Advanced Research in Fluid Mechanics and Thermal Sciences, 81(2), 98–109.

[52] Soon, C. C., Ghazali, R., Chong, S. H., Shern, C. M., Sam, Y. M., & Yusof, A. A. (2019). Performance Evaluation of Fractional Order Pid and Sliding Mode Control with Optimization Tuning Access. International Journal of Recent Technology and Engineering, 8(2S8), 1448–1454.

[53] Lee, T., Lee, D., Song, B., & Baek, Y. S. (2019). Design and Control of a Polycentric Knee Exoskeleton Using an Electro-Hydraulic Actuator. Sensors, 20(1), 211.

[54] Tafazoli, S., De Silva, C. W., & Lawrence, P. D. (1998). Tracking control of an electrohydraulic manipulator in the presence of friction. IEEE Transactions on Control Systems Technology, 6(3), 401–411.

[55] Su, Q., Pei, Z., Tang, Z., & Xie, H. (2020). Variable Structure Compensation PID Control for Lower Extremity Exoskeleton. Proceedings of the 15th IEEE Conference on Industrial Electronics and Applications, ICIEA 2020, 1544–1549.

[56] Kumar, J., Azar, A. T., Kumar, V., & Rana, K. P. S. (2018). Design of Fractional Order Fuzzy Sliding Mode Controller for Nonlinear Complex Systems. In Mathematical Techniques of Fractional Order Systems (pp. 249–282). Elsevier.

[57] Min, H. K., Sung, H. J., Lee, J. H., & Park, M. K. (2017, October). Robust control of electro-hydraulic load simulator using sliding mode control with perturbation estimation. In 2017 17th International Conference on Control, Automation and Systems (ICCAS) (pp. 1137-1141). IEEE.

[58] Knohl, T., & Unbehauen, H. (2000). Adaptive position control of electrohydraulic servo systems using ANN. Mechatronics, 10(1–2), 127–143.

[59] Feng, H., Ma, W., Yin, C., & Cao, D. (2021). Trajectory control of electro-hydraulic position servo system using improved PSO-PID controller. Automation in Construction, 127, 103722.

[60] Bessa, W. M., Dutra, M. S., & Kreuzer, E. (2010). Sliding mode control with adaptive fuzzy dead-zone compensation of an electro-hydraulic servo-system. Journal of Intelligent and Robotic Systems: Theory and Applications, 58, 3–16.

[61] Zhang, L., Cong, D., Yang, Z., Zhang, Y., & Han, J. (2016). Robust Tracking and Synchronization of Double Shaking Tables Based on Adaptive Sliding Mode Control with Novel Reaching Law. IEEE Access, 4, 8686–8702.

[62] Cheng, C., Liu, S., & Wu, H. (2020). Sliding mode observer-based fractional-order proportional–integral–derivative sliding mode control for electro-hydraulic servo systems. Proceedings of the Institution of Mechanical Engineers, Part C: Journal of Mechanical Engineering Science, 234(10), 1887–1898.

[63] Li, M., Shi, W., Wei, J., Fang, J., Guo, K., & Zhang, Q. (2019). Parallel velocity control of an electro-hydraulic actuator with dual disturbance observers. IEEE Access, 7, 56631-56641.

[64] Ji, X., Wang, C., Zhang, Z., Chen, S., & Guo, X. (2021). Nonlinear adaptive position control of hydraulic servo system based on sliding mode back-stepping design method. Proceedings of the Institution of Mechanical Engineers, Part I: Journal of Systems and Control Engineering, 235(4), 474-485.

[65] Rahmani, M., Ghanbari, A., & Ettefagh, M. M. (2016). Robust adaptive control of a bio-inspired robot manipulator using bat algorithm. Expert Systems with Applications, 56, 164–176.

[66] Liu, J., & Wang, X. (2011). Advanced Sliding Mode Control for Mechanical Systems (Vol. 74, Issue 1934). Springer Berlin Heidelberg.